CALIBRATION AND TESTING OF DISCRETE ELEMENT MODEL PARAMETERS FOR GIANT JUNCAO STEMS
/
巨菌草茎秆离散元模型参数标定与试验

Jianchao ZHANG[1,2], Yuanze SUN[1], Qi ZHAO[3]
[1]College of Mechanical and Electrical Engineering, Inner Mongolia Agricultural University / China
[2]Inner Mongolia Engineering Research Center of Intelligent Equipment for the Entire Process of Forage and Feed Production/ China
[3] College of Mechanical Engineering, Inner Mongolia University of Technology / China
Tel: 86-0471-17611417277; E-mail: luckxiaoqi@126.com
Corresponding author: Qi-ZHAO
DOI: https://doi.org/10.35633/inmateh-77-125

Keywords: giant Juncao stems, angle of repose, discrete element, numerical simulation, parameter calibration

ABSTRACT
To improve the accuracy of numerical simulations of the rolling process of giant Juncao stems using the discrete element method, this study focuses on the giant Juncao stems. In conjunction with physical experiments on giant Juncao stems and discrete element simulation methods, the Hertz-Mindlin with Bonding model is selected to establish a bonding model, and the parameters of the discrete element model are calibrated. The relative error between the numerical simulation's angle of repose and the angle of repose from physical experiments is used as an evaluation index. The Plackett-Burman test, Steepest Ascent test, and Box-Behnken test are designed to optimize the relevant parameters. The optimal parameter combination obtained includes a static friction coefficient between stems of 0.25, a rolling friction coefficient of 0.42, and a static friction coefficient between the stem and the steel plate of 0.52; the average angle of repose is 18.032°. Validation simulation tests are conducted with this parameter combination, resulting in a relative error of 1.1% between the obtained angle of repose and that from physical experiments. This indicates that the calibrated parameter results for the giant Juncao stems can be used for discrete element numerical simulation of crushing studies.

摘要
为解决据巨菌草短茎埋栽种植时的排种技术需求，研究旨在设计符合巨菌草茎秆物理特性的排种器。本研究结合巨菌草茎秆物理试验和离散元仿真方法，选用 Hertz-Mindlin with Bonding 模型建立粘结模型，对离散元模型参数进行标定。将数值模拟休止角和物理试验休止角的相对误差作为评价指标，设计 Plackett-Burman 试验、Steepest Ascent 试验和 Box-Behnken 试验对相关参数进行优化。获得最优参数组合：茎秆间静摩擦因数 0.25、滚动摩擦因数 0.42、茎秆与钢板静摩擦因数 0.52；休止角平均值为 18.032°。以此参数组合进行验证仿真试验，得到的休止角与物理试验休止角的相对误差为 1.1%。以上表明，建立的巨菌草茎秆标定参数结果可用于离散元数值模拟粉碎仿真研究。

INTRODUCTION
Giant Juncao grass is characterized by high nutritional value, strong stress resistance, wide environmental adaptability, and remarkably high biomass yield, and thus has considerable economic and ecological value *(Lin et al., 2003; Hayat et al, 2020)*. After being processed by kneading or ensiling, it becomes an ideal roughage source for ruminants. And the crushing performance is crucial for the efficient utilization of giant Juncao as feed *(Bai et al., 2021)*. To improve the knead performance of hammer-type machines, it is necessary to conduct numerical analyses of the crushing process of giant Juncao stems. However, the kneading process is completed inside the machine chamber, it is difficult to obtain the underlying mechanism associated with kneading silk of giant Juncao *(Huan et al., 2022; Zhao, 2024)*. The Discrete Element Method (DEM) is a numerical technique used to simulate and analyze the behavior of granular and particulate media under external forces. Due to its advantages in high-fidelity simulation, dynamic behavior analysis, and strong flexibility and adaptability, DEM has been widely applied in agricultural mechanization research *(Li et al., 2025)*. By applying DEM to simulate the crushing process of giant Juncao stems, the loading conditions of key components as well as the fracture behavior of the stems can be reproduced, which in turn significantly affects subsequent processing operations and overall crushing performance *(Zhang et al., 2020)*. Therefore, accurately determining the parameters required for DEM-based numerical models is of critical importance.

At present, researchers have carried out extensive studies on the calibration of DEM simulation parameters for plant stems. For agricultural materials such as forage, the construction and parameterization of DEM models are predominantly based on multi-sphere packing. Flexible particles are typically modeled in EDEM using the bond model, and the contact interactions between particles are most commonly described by the Hertz–Mindlin with bonding model *(Jiang, et al., 2024)*, the Hertz–Mindlin with JKR Cohesion (JKR) model *(Sher et al., 2021)*, or the Edinburgh Elasto-Plastic Adhesive (EEPA) model *(Paulick et al., 2015*). *Du et al. (2024)* measured the relevant mechanical parameters of tea stems and established a three-layer DEM model of tea stems based on an enhanced bonding approach. And the calibration parameters were used to construct the tensile and puncture models for the corresponding simulation experiments to optimize the tea stem harvesting process. Other scholars have employed DEM to calibrate the contact and material parameters of forage rape stems *(Xie et al., 2024)*, alfalfa stems *(Wang et al., 2025)*, notoginseng stems *(Xie et al., 2024), and sugarcane stems (Yang et al., 2025).*

In summary, previous studies have demonstrated the feasibility of using DEM to calibrate simulation parameters for stem-type crops. However, there are still relatively few studies focusing on the giant Juncao stems. Therefore, in this study, giant Juncao stems were selected as the research object, and combines physical test with simulation test. A bonded-particle model of giant Juncao stems was developed using the Hertz–Mindlin with Bonding contact model, and Plackett–Burman, Steepest Ascent, and Box–Behnken experimental designs were conducted to obtain the optimal parameter combination. The accuracy of the calibrated physical parameters was then verified by simulating the angle of repose. The results provide a reliable set of parameters for the DEM-based numerical simulation of the crushing process of giant Juncao stems.

MATERIALS AND METHODS

Materials

The experimental material was mature giant Juncao harvested from the East Campus plantation of Inner Mongolia Agricultural University. Robust and straight plants were selected to prepare stem samples. After cutting, 100 representative stem samples were randomly selected, and the length was carried out using the five-point method in accordance with GB/T 5262–2008 *(Hao et al., 2008)* by Vernier caliper. It showed that the stem size ranged from 130 to 150 mm, the major axis from 16 to 22 mm, and the minor axis from 14 to 20 mm. The moisture content was determined using a DHG-9140A electric thermostatic drying oven, and the average moisture content was 73.4%.

Fig. 1 - Giant Juncao stems

Determination of contact parameters of Giant Juncao stems

Determination of the static friction coefficient

The static friction coefficient is defined as the ratio of the maximum static friction force to the force acting on the contact surface. In this study, the static friction coefficients were determined between giant Juncao stems, and between giant Juncao stems and 45# steel.

First, the base of the inclined plane apparatus was adjusted to a horizontal position. The measurement plane was then rotated slowly until the giant Juncao stem began to slide on the steel plate. At this state, the inclination angle of the plane was recorded using an angle gauge, and the static friction coefficient between the giant Juncao stem and the steel plate was calculated using Eq. (1). The test was repeated 10 times, and the static friction coefficient ranged from 0.30 to 0.50.

$$f_s = \tan \alpha_1 \tag{1}$$

where: f_s is the static friction coefficient between the giant Juncao stem and the steel plate, α_1 is the critical angle of static friction coefficient (°).

Multiple stems of similar length and diameter were selected and fixed onto the inclined plane apparatus using adhesive tape, and the stems were positioned with their axes perpendicular to the fixed stems.

The inclined plane was slowly raised until the stem began to slide. The inclination angle displayed on the angle gauge was recorded as the critical angle. The test was repeated 10 times, and the resulting static friction coefficient ranged from 0.20 to 0.40.

Determination of the rolling friction coefficient

The rolling friction coefficient refers to the resistance to rolling caused by deformation at the contact surface when one object rolls without slipping, or shows an obvious tendency to roll. In this study, the rolling friction coefficients between giant Juncao stems and 45# steel, and between giant Juncao stems, were determined. The giant Juncao stems were used as a slider and placed on the steel plate of the inclined plane apparatus. As the inclined plane was slowly raised, the inclination angle at which the stem started to roll was recorded with an angle gauge. The measurement principle is illustrated in Figure 2. A force analysis was carried out at the moment when the stem exhibited a tendency to roll. After 10 repeated tests, the rolling friction coefficient between the giant Juncao stem and the steel plate ranged from 0.30 to 0.60.

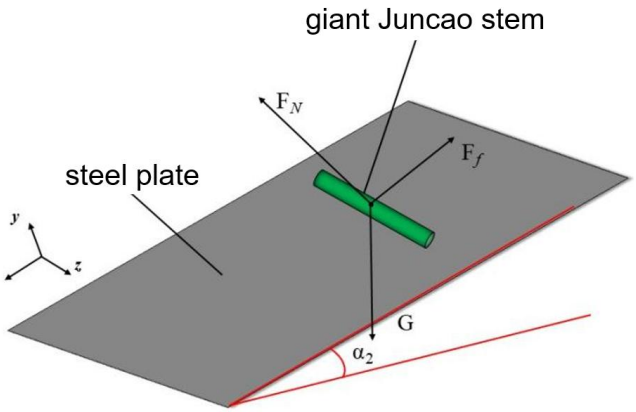

Fig. 2 - Measurement of the rolling friction coefficient between seed stems and steel plate

$$Fr = f\ F_N \quad (2)$$

$$F_N - G\cos\alpha_2 = 0 \quad (3)$$

$$Gr\sin\alpha_2 - Fr = 0 \quad (4)$$

$$f = \frac{Fr}{F_N} = r_0 \tan\alpha_2 \quad (5)$$

where:

Fr is the rolling friction (N); f is the rolling friction coefficient (dimensionless); F_N is the force exerted by the inclined plane on the stem (N); G is the gravitational force acting on the stem (N); α_2 is the critical angle for the onset of rolling (°), r_0 is the maximum radius of the stem (mm).

The giant Juncao stems were used as the test specimen. Several stems with similar length and diameter were selected and fixed onto the inclined plane apparatus with adhesive tape, with the sample stem placed parallel to the axis of the fixed stems. The inclined plane was then slowly raised until the stem began to roll, at which point the inclination angle displayed by the angle gauge was recorded as the critical angle for rolling. The rolling friction coefficient between stems ranged from 0.30 to 0.50.

Determination of the coefficient of restitution

The coefficient of restitution is a key parameter characterizing an object's ability to recover its original state after collisional deformation. Its mathematical expression is the ratio of the instantaneous normal separation velocity at the end of contact to the normal approach velocity before impact. The measurement principle is illustrated in Figure 3.

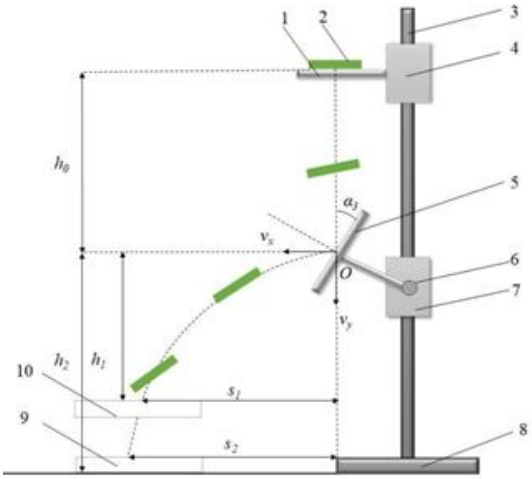

Fig. 3 - Schematic diagram of the coefficient of restitution

1 – stem drop reference plane; 2 – giant Juncao stem; 3 – support frame; 4 and 7 – adjustable bracket; 5 – impact plate; 6 – angle-adjusting nut for the impact plate; 8 – support base; 9 and 10 – receiving trays at different heights

The giant Juncao stem is released from a reference plane at a height h_0 above the impact plate and falls freely to collide with the plate. The plate material can be replaced according to experimental requirements, and the plate angle can be adjusted. Neglecting air resistance, the stem is subjected only to gravity during the descent. The instantaneous velocity of the giant Juncao stem before impact can be expressed as:

$$\begin{cases} v_1 = gt \\ h_0 = \dfrac{1}{2} gt^2 \end{cases} \tag{6}$$

where: v_1 is the pre-impact velocity of the Juncao stem (m/s), t is the free-fall time (s).

From Equation (6), the instantaneous velocity of the giant Juncao stem before impact with the impact plate is:

$$v_1 = \sqrt{2gh_0} \tag{7}$$

Assuming the rebound motion of the stem after impact is a level throw movement, the horizontal motion is uniform straight-line motion, and the vertical motion is uniformly accelerated motion. Treating the stem as a uniform geometry, the trajectory of the stem after rebound is given by:

$$\begin{cases} s = v_x t_0 \\ h = v_y + \dfrac{1}{2} g{t_0}^2 \end{cases} \tag{8}$$

where: t_0 is rebound motion time of the stem (s); s is horizontal displacement of the stem (m), h_0 is vertical fall distance after collision (m).

The rebound trajectory of the Juncao stem was captured using high-speed cameras under two different receiving-tray height conditions. The corresponding horizontal displacements s_1 and s_2, as well as the vertical displacements h_1 and h_2, were measured. The horizontal and vertical velocities of the Juncao stem were then calculated using Equation (9).

$$\begin{cases} v_x = \sqrt{\dfrac{g s_1 s_2 (s_1 - s_2)}{2(h_1 s_2 - h_2 s_1)}} \\ v_y = \dfrac{h_1 v_x}{s_1} - \dfrac{g s_1}{2 v_x} \end{cases} \tag{9}$$

According to the collision recovery coefficient, the calculation formula is:

$$e = \frac{v_n}{v_{0n}} = \frac{\sqrt{v_x^{\,2} + v_y^{\,2}}\cos(\alpha_3 + \arctan\frac{v_y}{v_x})}{v_0 \sin\alpha_3} \tag{10}$$

where: e is the coefficient of restitution; v_{0n} is the component of the pre-collision velocity (m/s); v_n is the component of the post-collision velocity (m/s); α_3 is the inclination angle of the collision plate (°).

Giant Juncao stems with similar diameters and lengths were uniformly affixed to the collision plate, and the previously described experimental procedure was repeated to determine the coefficient of restitution between stems. The coefficient of restitution for stem–stem collisions of giant Juncao ranged from 0.3 to 0.5, whereas that for stem–steel collisions ranged from 0.4 to 0.6.

Determination of the Poisson's ratio and shear modulus

Poisson's ratio is the absolute value of the ratio between the radial strain and the axial strain produced in a material under uniaxial tension or compression. This coefficient represents the elastic constant governing the material's transverse deformation. The Poisson's ratio for giant Juncao stem is measured using the definition method, and calculated by Equation (11).

$$\mu = \left|\frac{\varepsilon_x}{\varepsilon_y}\right| \tag{11}$$

where: μ is the Poisson's ratio; ε_x is the radial strain; ε_y is the axial strain.

A texture instrument was used to perform compression tests. The loading speed was set to 0.5 mm/s and the loading time to 15 s. After loading, a vernier caliper was used to measure the radial and axial deformations of the giant Juncao stem, and five repeated tests were conducted. Based on Eq. (11), the Poisson's ratio of the giant Juncao stem was calculated to range from 0.3 to 0.5.

In this study, the elastic modulus was measured using the three-point bending method, and the shear modulus was then derived accordingly. As shown in Fig. 4, a stem of 100 mm long was placed on the test bench, and a load was applied at the midpoint of the span. When the stress–strain response exhibited a cliff-like drop, the magnitude of the applied load was recorded by the testing machine program.

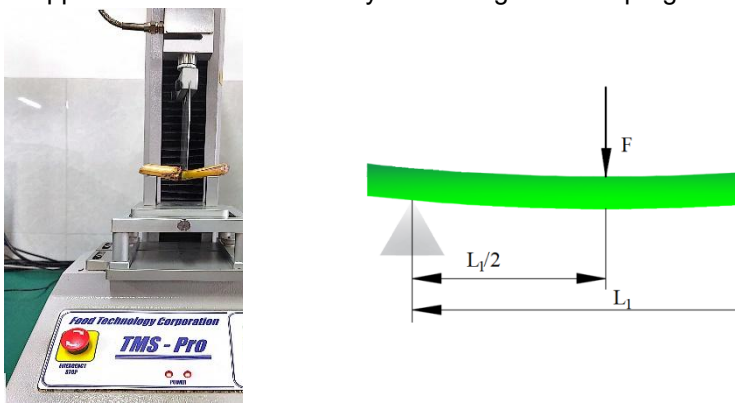

Fig. 4 - Three-point bending test and schematic diagram of the principle

The calculation formula for the flexural elastic modulus of giant Juncao is:

$$E = \frac{L_1^{\,3} F_b}{48\delta I} \tag{12}$$

where:

E is the elastic modulus (MPa); F_b is the applied load (N); L_1 is the span between the two supports (mm), I is the inertial moment (mm^4).

$$I = \frac{\pi d^{\,4}}{64} \tag{13}$$

where: d is the average diameter of the stem at the loading point (mm).

The deflection δ of the center point of the stem is calculated by Equation (14).

$$\delta = \frac{\pi d^3}{32} \tag{14}$$

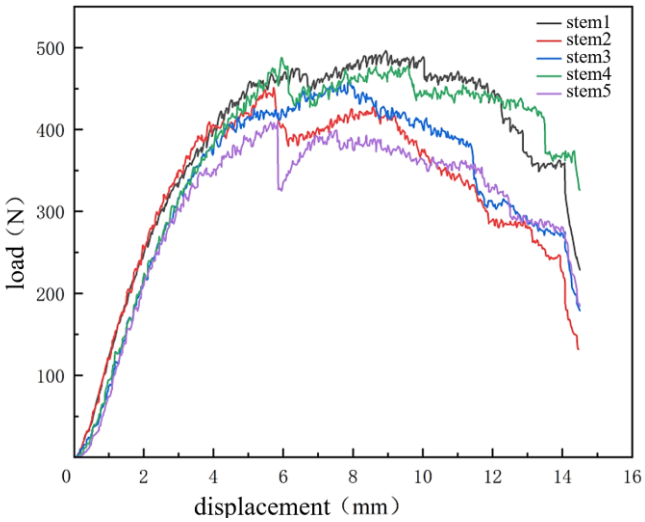

Fig. 5 - Load–displacement curve of the stem

As shown in Fig. 5, the variation trend of the load with deformation for five selected stems was obtained, from which the average elastic modulus was carried out. The shear modulus is the ratio of shear stress to shear strain for a material subjected to shear stress within the proportional limit of elastic deformation. It characterizes the material's resistance to shear deformation. The shear modulus G can be calculated by Eq.(15).

$$G = \frac{E}{2(1+\mu)} \tag{15}$$

Based on the bending test, the shear modulus of giant Juncao stem ranged from 280 to 480 MPa.

Physical measurement test of the angle of repose

The angle of repose is a key parameter for evaluating the flowability and frictional characteristics of materials. In this study, the sidewall collapse method was used to measure the angle of repose of giant Juncao stem. Sixty stems with similar lengths were selected and placed in a specially designed box. Both the outer walls and the central baffle of the box were made of transparent plastic panels to clearly observe the flow behavior of the stems. The test was repeated 10 times. After the stems formed a stable pile and the angle was established in each trial, photographs were taken.

MATLAB was used to convert the images to grayscale and then perform binary thresholding to enhance image contrast. Finally, the extracted contour boundary was fitted with an appropriate function curve to obtain the tangent of the angle of repose. As shown in Fig. 6, the angle of repose was 18.233°.

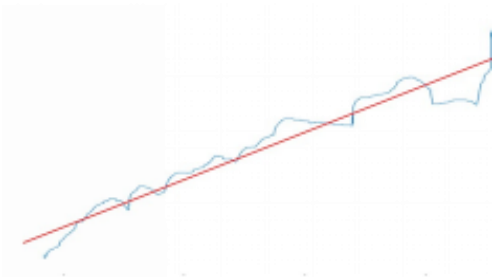

Fig. 6 - Angle of repose

Establishment of the DEM model

A stem simulation model with the corresponding dimensions was developed in EDEM, as shown in Fig. 7. The Hertz–Mindlin with bonding contact model was adopted, and the DEM model was constructed using the bonded-sphere approach to conduct the angle-of-repose simulation test.

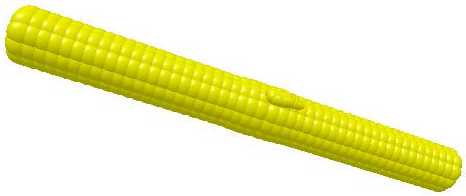

Fig. 7 - Stem DEM simulation model

As shown in Fig. 8, the box used for measuring the angle of repose was imported, and the corresponding material properties and contact parameters were assigned. A particle factory was added to generate 60 giant Juncao stems statically during 0 to 0.3 s. After the stem pile reached a stable state, an upward motion was applied to the central baffle at 0.3 s, causing the piled stems to collapse under gravity and form the angle of repose. The total simulation time was set to 1 s.

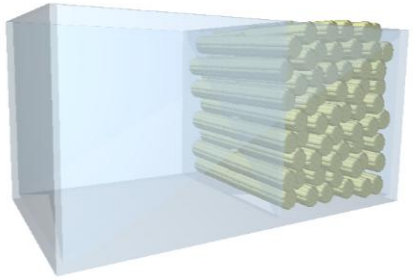

Fig. 8 - Angle-of-repose simulation test

RESULTS

Screening of influencing parameters for the angle of repose

As shown in Table 1, the parameters that affect the simulated physical behavior of giant Juncao stems were selected as experimental factors, with the angle of repose used as the evaluation index. A Plackett–Burman design was employed for the simulation experiments.

Table 1

Factor coding for Plackett-Burman test of physical parameters

Factor	coding	
	-1	1
Poisson's ratio of the stem x_1	0.3	0.5
Shear modulus of the stem x_2 (MPa)	280	480
Static friction coefficient (stem–stem) x_3	0.2	0.4
Rolling friction coefficient (stem–stem) x_4	0.3	0.5
Coefficient of restitution (stem–stem) x_5	0.3	0.5
Static friction coefficient (stem–steel plate) x_6	0.3	0.6
Rolling friction coefficient (stem–steel plate) x_7	0.3	0.6
Coefficient of restitution (stem–steel plate) x_8	0.4	0.6

The Plackett–Burman design and result is shown in Table 2.

Table 2

The Plackett–Burman design and result

Run	Factor								Angle of repose
	x_1	x_2	x_3	x_4	x_5	x_6	x_7	x_8	
1	0.5	480	0.2	0.5	0.5	0.6	0.3	0.4	20.57
2	0.3	480	0.4	0.3	0.5	0.6	0.6	0.4	15.11
3	0.5	280	0.4	0.5	0.3	0.6	0.6	0.6	20.53

Run	Factor								Angle of repose
	x_1	x_2	x_3	x_4	x_5	x_6	x_7	x_8	
4	0.3	480	0.2	0.5	0.5	0.3	0.6	0.6	23.51
5	0.3	280	0.4	0.3	0.5	0.6	0.3	0.6	17.72
6	0.3	280	0.2	0.5	0.3	0.6	0.6	0.4	18.07
7	0.5	280	0.2	0.3	0.5	0.3	0.6	0.6	21.24
8	0.5	480	0.2	0.3	0.3	0.6	0.3	0.6	14.04
9	0.5	480	0.4	0.3	0.3	0.3	0.6	0.4	22.44
10	0.3	480	0.4	0.5	0.3	0.3	0.3	0.6	29.66
11	0.5	280	0.4	0.5	0.5	0.3	0.3	0.4	28.49
12	0.5	280	0.2	0.3	0.3	0.3	0.3	0.4	19.62

The numerical simulation results were analyzed for significance using Design-Expert 13.0, as shown in Table 3.

Table 3

The Plackett–Burman design and result

Source	Sum of squares	df	Mean square	*F*-value	*P*-value	Significance
model	254.41	8	31.8	10.16	0.0413	
x_1	0.5461	1	0.5461	0.1745	0.7042	
x_2	0.0432	1	0.0432	0.0138	0.9139	
x_3	26.88	1	26.88	8.59	0.061	*
x_4	83.85	1	83.85	26.8	0.014	*
x_5	0.124	1	0.124	0.0396	0.8549	
x_6	133.2	1	133.2	42.57	0.0073	**
x_7	8.77	1	8.77	2.8	0.1926	
x_8	0.9976	1	0.9976	0.3188	0.6118	
residual	9.39	3	3.13			

Based on the significance test results of the Plackett–Burman for the physical parameters, the stem–stem static friction coefficient x_3, the stem–stem rolling friction coefficient x_4, and the stem–steel plate static friction coefficient x_6 had significant effects on the angle of repose, whereas the remaining parameters had relatively minor effects. Therefore, these three parameters were selected as experimental factors, and the angle of repose and the relative error of the simulated angle of repose with respect to the physical value were used as evaluation indices to conduct a steepest ascent test. For the parameters with minor effects, the intermediate levels of the values obtained from physical measurements were adopted. The steepest ascent test and the corresponding results are shown in Table 4.

Table 4

Steepest ascent test and results for physical parameters

Run	Factor			Angle of repose (°)	Relative error （%）
	x_3	x_4	x_6		
1	0.2	0.3	0.3	22.2	21.78
2	0.25	0.35	0.375	19.23	5.49
3	0.3	0.4	0.45	18.78	3.01
4	0.35	0.45	0.525	16.7	8.4
5	0.4	0.5	0.6	14.81	18.73

The test results showed that, in Run 3, the relative error is minimum. This indicates that the optimal parameter range lies near the factor levels of Run 3. Therefore, the factor levels of Run 3 were precisely defined as the center point, with the factor levels of Run 2 set as the low level and those of Run 4 set as the high level. The Box–Behnken test on the factor level was established to optimal combination of physical parameters. The results are shown in Table 5.

Table 5

Box–Behnken test and results for physical parameters

Run	Factor			Angle of repose (°)	Relative error （%）
	x_3	x_4	x_6		
1	0.25	0.35	0.45	16.75	8.11
2	0.35	0.35	0.45	17.8	2.38
3	0.25	0.45	0.45	18.07	0.88
4	0.35	0.45	0.45	15.64	14.19
5	0.25	0.4	0.375	19.07	4.61
6	0.35	0.4	0.375	18.37	0.77
7	0.25	0.4	0.525	17.98	1.37
8	0.35	0.4	0.525	16.44	9.84
9	0.3	0.35	0.375	19.19	5.25
10	0.3	0.45	0.375	16.71	8.34
11	0.3	0.35	0.525	17.21	5.59
12	0.3	0.45	0.525	15.91	12.74
13	0.3	0.4	0.45	18.88	3.57
14	0.3	0.4	0.45	18.79	3.07
15	0.3	0.4	0.45	18.85	3.4
16	0.3	0.4	0.45	18.76	2.91
17	0.3	0.4	0.45	18.82	3.24

An ANOVA was performed on the Box–Behnken experimental results for the physical parameters using Design-Expert 13.0, and the results are shown in Table 6.

Table 6

The Plackett–Burman design and result

Source	Sum of squares	df	Mean square	*F*-value	*P*-value	Significance
model	11.33	9	1.26	33.13	< 0.0001	**
x_3	1.84	1	1.84	48.49	0.0002	**
x_4	2.22	1	2.22	58.28	0.0001	**
x_6	1.97	1	1.97	51.82	0.0002	**
x_3 x_4	1.99	1	1.99	52.30	0.0002	**
x_3 x_6	0.1089	1	0.1089	2.86	0.1344	
X_4 x_6	0.9506	1	0.9506	25.01	0.0016	**
x_3^2	0.5756	1	0.5756	15.14	0.0060	**
x_4^2	1.48	1	1.48	38.85	0.0004	**

Source	Sum of squares	df	Mean square	*F*-value	*P*-value	Significance
x_6^2	0.0440	1	0.0440	1.16	0.3176	
residual	0.2661	7	0.0380			
Lack of Fit	0.1958	3	0.0653	3.72	0.1186	
Pure Error	0.0703	4	0.0176			
Total	11.60	16				

The results indicate that: x_3, x_4, x_6, x_3x_4, x_3^2 and x_4^2 have significant effects on the angle of repose, whereas x_3x_6, x_4x_6 and x_6^2 do not. The fitted regression model for the angle of repose is significant, and the lack-of-fit is not significant. The coefficient of determination is R^2=0.9457, and the coefficient of variation is 2.31%, suggesting that the model can accurately reflect the actual situation and can be used to predict the angle of repose. Accordingly, a second-order regression equation relating the simulated angle of repose of giant Juncao stems to the three significant parameters was obtained (Eq. (16)).

$$\theta_1 = -114.315 + 280.75x_3 + 451.85x_4 + 28.867x_6 - 348x_3x_4 - 56x_3x_6 + 78.67x_4x_6 - 209x_3^2 - 493x_4^2 - 59.11x_6^2 \quad (16)$$

Using the optimization module in Design-Expert 13.0, the regression was optimized, yielding the optimal combination of x_3, x_4 and x_6 as 0.25, 0.42, and 0.52, respectively. The predicted angle of repose was 18.062°, with a relative error of 0.94% compared with the mean value from the physical tests. Which indicate that the regression prediction model for the angle of repose of giant Juncao stems is sufficiently accurate.

Result of verification test

To verify the accuracy and feasibility of the calibrated physical parameters, simulation tests of the angle of repose for giant Juncao stems were conducted. The optimal combination of the significant parameters was adopted, while the non-significant parameters were set to the mid-range values measured in the physical tests. The results showed that the mean simulated angle of repose was 18.032°, and the relative error with respect to the mean value from the physical tests was only 1.1%. This confirms that the calibrated parameters for giant Juncao stems are accurate and feasible, and can provide reliable data support for subsequent research and applications. A comparison between the physical and numerical simulation tests of the angle of repose is shown in Fig. 9.

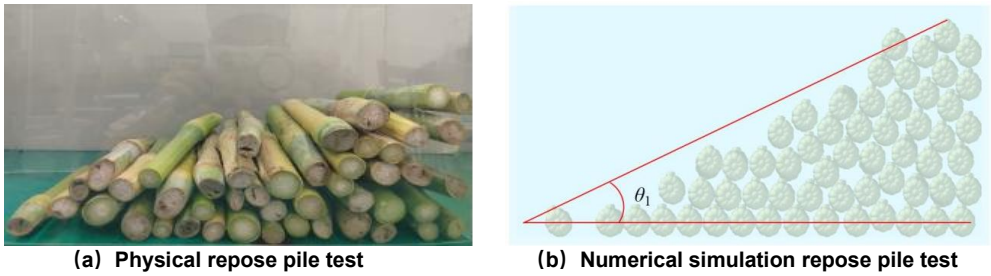

(a) Physical repose pile test (b) Numerical simulation repose pile test

Fig. 9 - Comparison of physical and numerical simulation for the angle of repose

CONCLUSIONS

(1) Physical tests showed that the Poisson's ratio of giant Juncao stems ranged from 0.3 to 0.5, and the shear modulus ranged from 280 to 480 MPa. The static friction coefficient ranged from 0.3 to 0.5 between stems and a steel plate and from 0.2 to 0.4 between stems. The rolling friction coefficient ranged from 0.3 to 0.6 between stems and a steel plate and from 0.3 to 0.5 between stems. The coefficient of restitution was measured to be 0.4 to 0.6 between stems and a steel plate and 0.3–0.5 between stems.

(2) Based on the EDEM discrete element simulation software, the Hertz–Mindlin with bonding contact model was used to calibrate the contact parameters of giant Juncao stems. According to the significance test results of the Plackett–Burman test for physical parameters, the static friction coefficient between stems, rolling friction coefficient between stems, and static friction coefficient between stems and a steel plate had significant effects on the angle of repose.

(3) Through simulation tests on giant Juncao stems, screening of influential parameters for the angle of repose, the steepest ascent test, and the Box–Behnken test, a fitted regression equation for the angle of repose was obtained and an optimal solution was determined: static friction coefficient between stems of 0.25, rolling friction coefficient between stems of 0.42, and static friction coefficient between stems and a steel plate of 0.52. The mean simulated angle of repose was 18.032°, with a relative error of 1.1% compared with the measured physical test value of 18.233°, confirming the reliability of the calibrated simulation parameters.

ACKNOWLEDGEMENT

This study was supported by the National Natural Science Foundation of China (32560833), and Inner Mongolia Autonomous Region Natural Science Foundation (2025LHMS03020)). Research Program of science and technology at Universities of Inner Mongolia Autonomous Region (NJZZ23047), Program for improving the Scientific Research Ability of Youth Teachers of Inner Mongolia Agricultural University (BR230154).

REFERENCES

[1] Bai, S.H., Yang, Q.Z., Niu, K., Zhao, B., Zhou, L.M., Yuan, Y.W. (2021). Discrete Element-Based Optimization Parameters of an Experimental Corn Silage Crushing and Throwing Device. *Transactions of the ASABE,* 64(3), 1019-1026.

[2] Du, Z., Li, DD.H., Li, X.P., Jin X., Wu, Y.B., Yu F. (2024). Calibration and Experiment of Discrete Element Model Parameters for Tea Stem (茶茎秆离散元模型参数标定与试验) [J] *Transactions of the Chinese Society for Agricultural Machinery*, 56(1), 311-320.

[3] Hao, W.L., Liu, H.X., Zhu, L., Meng, Q.H. (2008). Agricultural Machinery Testing Conditions-General Rules for Measuring Methods (农业机械试验条件测定方法的一般规定) GB/T 5262-2008. *China Standards* Press.

[4] Hayat, K., Zhou, Y.F., Menhas, S., Bundschuh, J., Hayat, S., Ullah, A., Wang, J.C., Chen, X.F., Zhang, D., Zhou, P. (2020). Pennisetum giganteum: An emerging salt accumulating/tolerant non-conventional crop for sustainable saline agriculture and simultaneous phytoremediation. *Environment Pollution*, 265(PT A), 114876.

[5] Huan, X.L., Wang, D.C., You, Y., Ma, W.P., Zhu, L., Li, S.B. (2022). Establishment and Calibration of Discrete Element Model of King Grass Stalk Based on Throwing Test. *INMATEH - Agricultural Engineering*, 66(1), 19-137.

[6] Jiang, S.Y., Ren, D.Z., Ma, F., Chen, Z.Y., Che, Y.M.(2024) Parameter Calibration Of Rice Straw Particle-Crushing Model. *Engenharia Agricola*, 44, e20240063.

[7] Li, B., Li, F.L, Xia, C.L, Zhu, L, Cai, Z.Y., Wu, H. (2025). Design and Experiment of The Drum Baking Machine for Lu'an Guapian Tea Based on EDEM (基于 EDEM 的六安瓜片滚筒式烘焙机设计与试验) [J]. *Transactions of the Chinese Society of Agricultural Engineering*, 41(12), 310-321.

[8] Lin H. (2003). Juncao Science (菌草学) [M]. *China Agricultural Science and Technology Press*, 110-118.

[9] Paulick, M., Morgeneyer, M., Kwade, A. (2015). Review on The Influence of Elastic Particle Properties on DEM Simulation Results. *Powder Technology,* 283, 66-76.

[10] Sher, A., Yao, M., Li, Z., Farman A., Mazhar, H., Liang, Z., Kashif A. (2021). Discrete Element Method (DEM) Simulation of Single Grooser Shoe-Soil Interaction at Varied Moisture Contents. *Computers and Electronics in Agriculture*, 191, 106538.

[11] Wang, J.J., Geng, B.L., Yang, Z.K., Yang, J.L., Zhang, K.P., Meng, Y.R. (2025). Discrete Meta-Modeling and Parameter Calibration of Harvested Alfalfa Stalks. *Agronomy-Basel*, 15(10), 2390.

[12] Xie, K.T., Zhang, Z.G., Wang, F.A., Yu, X.L., Wang, C.L., Jiang, S.F. (2024). Calibration and Experimental Verification of Discrete Element Parameters of Panax Notoginseng Root, *International Journal Of Agricultural and Biological Engineering*, 17(4), 13-23.

[13] Xie, W., Ou, Y.C., Jiang, P., Meng, D.X., Luo, H.F. (2024). Calibrating and optimizing the discrete element parameters for clamping section stems during rape shoot harvesting (面向夹持采收的油菜薹夹段茎秆离散元参数标定与优化)[J]. *Transactions of the Chinese Society of Agricultural Engineering*, 40(7): 104-116.

[14] Yang, W., Yao, J.M., Zhang, D.B., Xi，J.H., Huang, Y., Lu, Z.H. (2025). Research on Discrete Element Modeling and Contact Parameter Calibration Methods for Complex Sugarcane Stalk Segments. *Sugar Tech*, 27(6), 1912-1924.

[15] Zhao, Y., Zhai, Z.P., Gao, B., Lan, Y.Z.(2024) Numerical Prediction and Optimization of Aerodynamic Noise of Straw Crushers by Considering The Straw-crushing Process. *Physics of Fluids*, 36(4), 043330.

[16] Zhang, T., Zhao, M.Q., Liu, F., Tian, H.Q., Wulan, T.Y., Yue, Y., Li, D.P. (2020). A Discrete Element Method Model of Corn Stalk and Its Mechanical Characteristic Parameters, *Bioresources*, 15(4), 9337-9350.